



AIAA 93-0096

**Flight Dynamics and Optimal Design of a Tethered Satellite
with wings in Free Molecular Flow**

A. Santangelo and V. Coppola

Department of Aerospace Engineering

The University of Michigan

Ann Arbor, Michigan

**31st Aerospace Sciences
Meeting & Exhibit**
January 11-14, 1993 / Reno, NV

FLIGHT DYNAMICS AND OPTIMAL DESIGN OF A TETHERED SATELLITE WITH WINGS IN FREE MOLECULAR FLOW

Andrew D. Santangelo‡ and Vincent T. Coppola†
 Department of Aerospace Engineering
 The University of Michigan, Ann Arbor, Michigan, U.S.A.

Abstract

We present an analysis of the attitude dynamics of the Tethered Satellite/Wing System (TS/WS) in free molecular flow (at an altitude of 142 km). The analysis indicates that a wing system could provide stable flight over a wide range of initial conditions.

Nomenclature

A	Eigenvector matrix
$\hat{\mathbf{b}}$	Body (principle) axes (x,y,z)
B	Reciprocal of most probable molecular speed, m/s
$\hat{\mathbf{c}}$	Orbiting Axes (r,θ,z)
C	Stream velocity, m/s
C'	Relative stream velocity, m/s
C	Most probable speed of emitted particles
C_D	Drag Coefficient
d	distance term, m
h	Altitude above the surface of the Earth, m
i	orbit inclination
I	Principle inertia dyadic of the TS/WS about the tether-TS/WS connection, kg•m ²
l	Direction cosine
l	length of a single flat plate wing, m
m	mass, total mass of the TS/WS, kg
M	moments, total moments about the tether-TS/WS connection, N•m
M	Mass flux, kg/(s•m ²)
P	Pressure, N/m ²
r	Position vector measured from <i>o</i> to a point, m
r	radius of a component, m
R	position vector from the origin of the inertial coordinate system to the tether-TS/WS connection, m
R	Altitude of the TS/WS from the origin of the Inertial coordinate system, m
R	Universal Gas Constant, J/(kg•k)
S	Area, m ²
Sr	Speed Ratio
T	Rotation matrix
T	Wall/Free Stream Temperature, k
t	Time, s
t	Wing thickness
U	Controllability matrix

U	Force function
u	Molecular thermal velocity, m/s
v	Velocity, m/s
v, v	Speed, m/s
v'	Relative velocity of the flow at a point w.r.t. inertial space, m/s
x	Euler angle vector
x,y,z	local coordinates in the body axes
α	Radius of the Earth, m
β,β',β''	Direction cosines
ζ	damping ratio
γ	Pitch Euler angle
φ	Roll Euler angle
ψ	Yaw Euler angle
κ	constant due to aerodynamic shadow effects
ρ	Density, kg/m ³
ρ	Position vector from the tether-TS/WS connection to the TS/WS center of mass, m
ω	Total angular velocity of the TS/WS w.r.t. inertial space
λ	Eigenvalue
ω	Frequency
Ω	Angular velocity of the Earth's atmosphere
μ⁰	Non-dimensional inertia tensor about the principle axes
μ	Geocentric gravitational constant, m ³ /s ²
θ	Angular position in the orbital plane

Subscripts

a	Atmosphere
b	Boom
cm	center of mass of orbiter-TS/WS
d	Drag
eq	Equilibrium
g	Gravity
i	impinging
k	keel
l	Euler angle, body axis index
m	maximum
o	orbiter, quantity at t=0
O	Designation of tether-TS/WS connection
p	Probe
r	re-impingement
s	Strut
ts/ws	Tethered satellite/wing system
w	wings
x,y,z	Value about either the x, y, or z-axes

Superscripts

O	Designation of tether-TS/WS connection
w	wings
x,y,z	Total value about either the x, y, or z-axes
ψ,φ,γ	Euler angles

‡Graduate Research Assistant, Department of Aerospace Engineering, Student Member AIAA

†Assistant Professor, Department of Aerospace Engineering

I. Introduction

In the mid to late 1990's, NASA and ASI (the Italian Space Agency) are tentatively planning a joint venture to explore the Earth's upper atmosphere and ionosphere using remote sensors housed in a satellite tethered from the Shuttle orbiter. One future mission, called TSS AVM (Tethered Satellite System Atmospheric Vehicle Mission), is to collect atmospheric information in the altitude range of 90-160 km, altitudes which cannot currently be explored using balloons or aircraft. This information is needed to better understand and model atmospheric phenomena including weather patterns, pollutant transmission, atmospheric chemistry, and ecosystem interactions. Moreover, the next generation of hypersonic vehicles are planning to fly through this atmospheric region.¹⁻⁴

The mission requires the main sensing probe on the TSS to point in the direction of the velocity vector within a tolerance of 2° during flight. Although active control methods have been proposed to meet this requirement, we propose to use a passive control consisting of a wing system connected to the spherical probe by a rigid boom/keel system (see fig. 1). The wings are designed to orient the probe into the direction of the velocity vector by creating a torque on the system from lift and drag from the atmospheric flow impinging on the wing; the keel structure is designed to hinder motion about the roll axis. We call this the Tethered Satellite/Wing System (TS/WS). The goal of this research is to find an optimal configuration for the TS/WS to assure stable flight.

In the preliminary conceptual model presented in reference 5, planar motion of the TS/WS was examined for flight in an ideal atmospheric environment. The preliminary analysis indicated that the wing system could provide stable flight over a wide range of conditions.

In early studies NASA examined the aerodynamic effects on the spherical part of the satellite and the connecting tether in rarefied hypersonic flow; also studied were conceptual models of a TSS wing system with a 45° half-angle cone frustum attached to a 1 m diameter spherical satellite. However, in both models no external loads were applied, stability analysis was not considered and model design optimization was not conducted. In the second model, a continuum flow model of the atmosphere was applied.^{6,7} More recently Dogra, Moss et. al. studied the aerothermodynamics and flow past a sphere

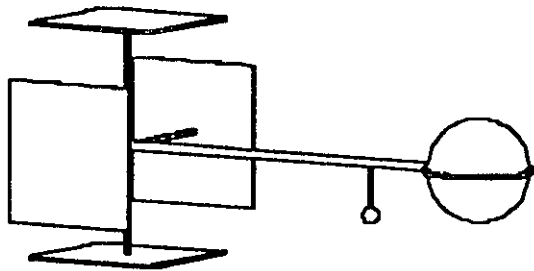


Fig. 1 Conceptual model of the TS/WS

using the direct simulation Monte Carlo (DSMC) method. In their work they determined not only the pressure, temperature and the structure of the flow over a sphere, but also found that transitional effects exist up to 200 km.^{8,9} Similarly, Dogra and Moss also examined *Hypersonic Rarefied Flow About Plates at Incidence*¹⁰, and similarly concluded again transitional effects exist up to altitudes of 200 km for plates of 12 m in length. They also derived various aerodynamic coefficients. Their results did show a relatively close correlation in the drag coefficient computed using the free molecular flow model and the DSMC method for large Knudsen number (~ 10).

Several authors have examined the aerodynamic effects on the orbiter-tether-probe, or dumbbell, configuration on the dynamics of the system. Puig-Suari and Longuski developed a dynamic model to study not only the behavior of the tethered system, but also its use in aerobraking.^{11,12} Fujii, et. al. studied the control of the deployment and retrieval of the dumbbell configuration.¹³ Shakhov studied a similar configuration using a smaller probe (mass = 1 kg). His study focused not only on linear oscillations but also weakly non-linear oscillations.¹⁴ Shakhov also treated the tether as a flexible structure, whereas references 11 - 13 treat the tether as a rigid rod.

II. Background

Much of the conceptual design and mission requirements of the Tethered Satellite spherical model have been posed. The TSS will be lowered to an altitude of 130 km where it will conduct its studies. Upon completion it will be further lowered until the tether breaks from heating or is severed from the shuttle. The probe has a mass of 500 kg and a diameter of 1.6 m.¹⁻³ Fig. 2 shows a detailed model of the TS/WS with design parameters used in the paper.

By examination of the proposed mission, it can be seen that the TS/WS, flying in tandem with the Space Shuttle orbiter at a speed of roughly 7,400 m/sec, will fly in a very low pressure atmosphere at "hypersonic" velocities where the Knudsen number is roughly 1 to 30 depending on the altitude. (The Knudsen number relates the ratio of the effective collision

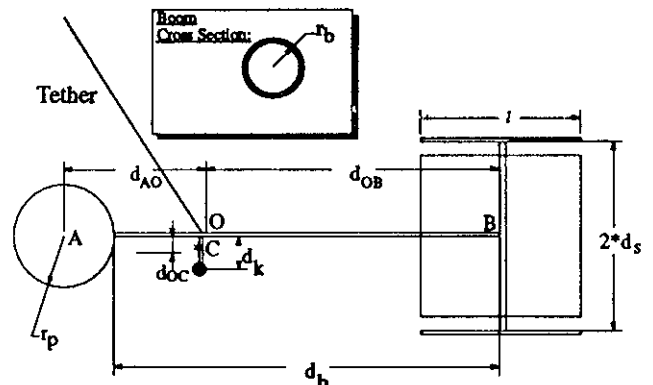


Fig. 2 Detailed model of the TS/WS with design parameters

mean free path to the size of the obstacle.) In this range of Knudsen number there are two regimes of flight that must be considered: collisionless or free molecular flow (>140 km), in which the collisions of the atmospheric molecules with each other have no effect on the force on the TS/WS, and transition flow (~ 100 km - 140 km), in which the collisions of atmospheric molecules with each other begin to effect the loads on the TS/WS. This paper will examine flight in free molecular flow. The free molecular flow was modeled by application of the kinetic theory of gases, or more specifically the Newtonian-Diffuse method.¹⁵⁻¹⁷

The wing derived here is based on square flat plate wings. The tether is connected to the TS/WS along the boom. Moreover, the keel structure is located so that center of mass lies along the keel's centerline. The wing and boom dimensions are constrained so that it will fit within the space shuttle cargo bay.¹⁸

It is further assumed that there will not be any active control of the wing position, the wing structure incorporates a protective coating to protect it from the hostile upper atmosphere and hypersonic velocities.

Optimization of the design to provide stable flight was completed through the use of two different computer applications. Each application was used to derive an optimal solution; once obtained the solutions were compared to provide further solution validation. The first method used was to conduct a parametric analysis and graphically view the results in the application *Mathematica*.¹⁹ The computer program *Optimum* which incorporates both the general conjugate gradient algorithm and the golden section acceptable point search algorithm was also used to conduct model optimization.²⁰

III. Model Development

The attitude dynamics of the TS/WS are modeled by Euler's equations for the rotational motion of a rigid body subject to torques generated by atmospheric drag and lift, and gravity. Other environmental torques are ignored. A model of the Tethered Satellite System with the coordinate systems defined is shown in fig. 3. The orbiting and body axes are related by

$$\hat{\mathbf{b}} = \mathbf{T} \hat{\mathbf{c}} \quad (1)$$

where the {132} Euler Angles (Ψ, γ, ϕ) are defined by the rotation matrix,

$$\mathbf{T} = \begin{bmatrix} c\gamma c\phi & c\phi s\gamma c\psi + s\phi s\psi & c\phi s\gamma s\psi - s\phi c\psi \\ -s\gamma & c\gamma c\psi & c\gamma s\psi \\ c\gamma s\phi & -c\phi s\psi + s\phi s\gamma c\psi & c\phi c\psi + s\phi \gamma c\psi \end{bmatrix} \quad (2)$$

($c\gamma = \cos \gamma$, $s\gamma = \sin \gamma$, etc.) Note that ψ measures the yaw, γ measures the pitch, and ϕ measures the roll. The axes align with $(\mathbf{e}_r, \mathbf{e}_\theta, \mathbf{e}_z)$ for $(\Psi, \gamma, \phi) = (0,0,0)$ so that the equilibrium is defined by $(\Psi, \gamma, \phi)_{eq} = (0,0,0)$.

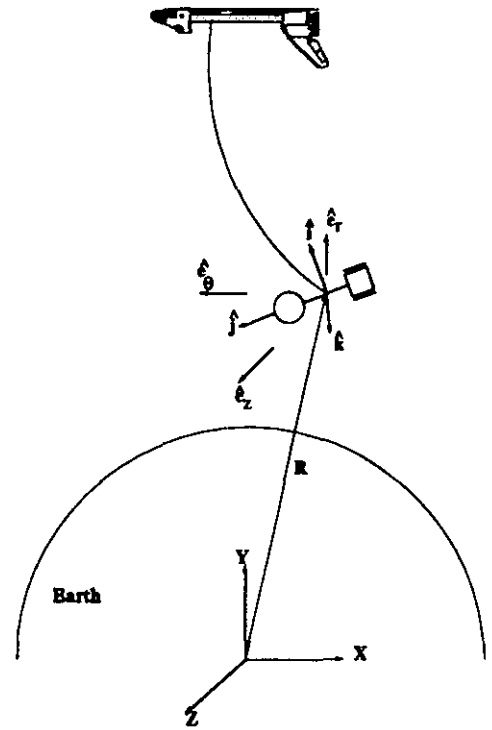


Fig. 3 Coordinate systems used in the analysis (drawing not to scale)

In this model we will assume the orbiter-TS/WS is in a circular orbit, where θ measures angular position in orbital plane and Earth oblateness is ignored. The the motion of the TS/WS is governed by the equation

$$I^O \dot{\omega} + \omega \times (I^O \omega) + m(\rho \times \ddot{\mathbf{R}}) = \mathbf{M} \quad (3)$$

where,

$$\rho = -d_{oc} \hat{\mathbf{i}} \quad (4)$$

$$\ddot{\mathbf{R}} = R \dot{\theta}^2 [-\hat{\mathbf{i}} + \gamma \hat{\mathbf{j}} - \phi \hat{\mathbf{k}}] \quad (5)$$

$$\omega = \dot{\psi} \hat{\mathbf{i}} + \dot{\phi} \hat{\mathbf{j}} + (\dot{\gamma} + \dot{\theta}) \hat{\mathbf{k}} \quad (6)$$

have been linearized about the equilibrium position defined by $(\Psi, \gamma, \phi)_{eq}$ and $(d\Psi/dt, d\gamma/dt, d\phi/dt) = (0,0,0)$. Note, excluding the "keel" structure it is assumed the TS/WS is symmetric about the y-axis and $I_{xx} = I_{zz}$. Calculating the acceleration term and linearizing the left hand side in eqn. (3) we get

$$I^O \dot{\omega} - m \rho R \dot{\theta}^2 [\phi \hat{\mathbf{j}} + \gamma \hat{\mathbf{k}}] = \mathbf{M} \quad (7)$$

Gravitational Moments

The moments derived from gravity gradient effects about the tether-TS/WS connection is approximated by²¹

$$\mathbf{M}_g = \hat{\mathbf{e}}_r \times \left[\frac{\partial U}{\partial \beta} \hat{\mathbf{i}} + \frac{\partial U}{\partial \beta'} \hat{\mathbf{j}} + \frac{\partial U}{\partial \beta''} \hat{\mathbf{k}} \right] \quad (8)$$

where,

$$U = \frac{\mu m}{R} - \frac{\mu m}{R^2} (x_{oc} \beta + y_{oc} \beta' + z_{oc} \beta'') + \frac{1}{2} \frac{\mu}{R^3} (I_{xx}^O + I_{yy}^O + I_{zz}^O) - \frac{3}{2} \frac{\mu}{R^3} (I_{xx}^O \beta^2 + I_{yy}^O \beta'^2 + I_{zz}^O \beta''^2) + \mathcal{O}\left(\frac{\mu^2}{R^4}\right) \quad (9)$$

and (β, β', β'') are defined by

$$\hat{\mathbf{e}}_r = \beta \hat{\mathbf{i}} + \beta' \hat{\mathbf{j}} + \beta'' \hat{\mathbf{k}} \quad (10)$$

Again, linearizing we get for the moments from gravity gradient effects about the tether-TS/WS connection

$$\mathbf{M}_g = 3 \frac{\mu}{R^3} \left[\left(I_{xx}^O - I_{zz}^O - \frac{m R d_{oc}}{3} \right) \hat{\mathbf{j}} + \left(I_{xx}^O - I_{yy}^O - \frac{m R d_{oc}}{3} \right) \gamma \hat{\mathbf{k}} \right] \quad (11)$$

Aerodynamic Moments

In developing the various aerodynamic coefficients it is assumed that the atmosphere rotates with the Earth, and \mathbf{v}_a is given by

$$\mathbf{v}_a = R \Omega \cos(i) \hat{\mathbf{e}}_\theta - R \Omega \sin(i) \cos(\theta) \hat{\mathbf{e}}_z \quad (12)$$

or

$$\mathbf{v}_a = [R \Omega \cos(i) \gamma + R \Omega \sin(i) \cos(\theta) \phi] \hat{\mathbf{i}} + [R \Omega \cos(i) - R \Omega \sin(i) \cos(\theta) \psi] \hat{\mathbf{j}} + [-R \Omega \cos(i) \psi - R \Omega \sin(i) \cos(\theta)] \hat{\mathbf{k}} \quad (12a)$$

where Ω represents the angular velocity of the atmosphere. Also the velocity of the TS/WS at "O" is given by the relationship

$$\mathbf{v}_O = R \hat{\theta} \hat{\mathbf{e}}_\theta \quad (13)$$

$$\hat{\theta} = \sqrt{\frac{\mu}{(\alpha + h_{cm})^3}} \quad (14)$$

Probe Drag Moments

The drag force on the spherical probe is given by

$$\mathbf{F}_{d_p} = \frac{1}{2} \rho_a C_{d_p} S_p v_{a/p} \nabla_{a/p} \quad (15)$$

where

$$\nabla_{a/p} = \nabla_{O/a} + \omega \times \mathbf{r}_p \quad (16)$$

and $v_{a/p}$ is the linearized speed. Because of the symmetry of the spherical probe, we will assume the center of pressure is

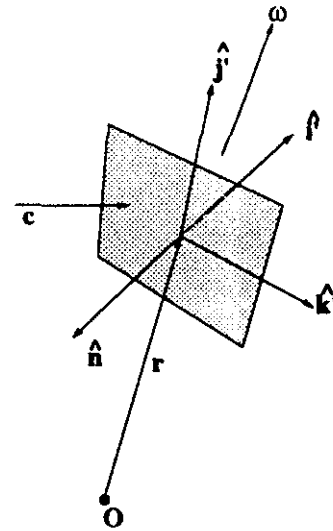


Fig. 4 Atmospheric molecules with absolute velocity \mathbf{C}_i impinging on an area element in free molecular flow.

always located at the forward edge of the probe and is directed parallel to the \mathbf{e}_θ -axis. Hence, using $(d_{AO} \hat{\mathbf{j}} + r_p \mathbf{e}_\theta)$ as the moment arm, we get the probe drag moment

$$\mathbf{M}_{d_p} = [r_p \gamma \hat{\mathbf{i}} + (d_{AO} + r_p) \hat{\mathbf{j}} - r_p \psi \hat{\mathbf{k}}] \times \mathbf{F}_{d_p} \quad (17)$$

Wing Aerodynamic Moments

Figure 4 shows an area element of a single flat plate wing in free molecular flow. The force per unit area from the impinging molecules on the flat plate wing is given by^{15,16}

$$\mathbf{P}_i^{front} = \rho_a \int_{-\infty}^{\infty} \int_{-\infty}^{\infty} \int_{-\infty}^{\infty} (\mathbf{C}_i \cdot \hat{\mathbf{n}}) (\mathbf{C}_i) f(\mathbf{C}_i - \mathbf{v}_{a/O} + \omega \times \mathbf{r}) d\mathbf{C}_i \quad (18a)$$

$$\mathbf{P}_i^{back} = -\rho_a \int_{-\infty}^{\infty} \int_{-\infty}^{\infty} \int_{-\infty}^{\infty} (\mathbf{C}_i \cdot \hat{\mathbf{n}}) (\mathbf{C}_i) f(\mathbf{C}_i - \mathbf{v}_{a/O} + \omega \times \mathbf{r}) d\mathbf{C}_i \quad (18b)$$

where

$$\mathbf{C}_i = \mathbf{v}_{a/O} - \omega \times \mathbf{r} + \mathbf{u} \quad (19)$$

and

$$f(\mathbf{C}_i - \mathbf{v}) = \frac{B^3}{\pi^{3/2}} \exp\{-B^2 (\mathbf{C}_i - \mathbf{v})^2\} \quad (20)$$

is the velocity distribution function in velocity space, where

$$B = \frac{1}{\sqrt{2RT}} \quad (21)$$

Note, the net force per unit area on the "back" or shadowed side of the plate is approximately 0. Hence, depending on the orientation of the TS/WS, either eqn (18a) or (18b) is the

active equation. To accurately account for the shadowing effect, each equation was first integrated. The resulting force per unit area for each side of each wing was then compared; it was noted that the pressure equations had the same coefficients, however some term's experienced sign changes. In order to model the pressure into one equation, the force per unit area for a wing is given by

$$P_f = \frac{\rho}{2 B^2 \sqrt{\pi}} \left[(I_x B v_{w/p,x} + I_y B v_{w/p,y} + I_z B v_{w/p,z})^* \left\{ \sqrt{\pi} B v_{w/p,z} (\text{sign}(\psi) + \text{erf}(B v_{w/p,z})) \right. \right. \\ \left. \left. + \exp(-B^2 v_{w/p,z}^2) \right\} + \frac{\sqrt{\pi}}{2} I_x (\text{sign}(\psi) + \text{erf}(B v_{w/p,z})) \right] \quad (22)$$

where the $\text{sign}(\psi)$ was utilized to account for the resulting sign change, depending on which side of the wing was being shadowed. Note, when $\psi = 0$, both sides of the wing are active, hence the net normal force is zero.

Besides the forces from the impinging molecules, we must also consider the forces from re-emission of molecules. Molecules can reflect from the plate either specularly (the molecule's angle of reflection is the same as the angle of incidence) or diffusely. Diffuse reflection implies the molecules are reflected randomly. In the model developed it is assumed the molecules undergo diffuse reflection with full surface accommodation, which is consistent with typical spacecraft surfaces. In diffuse reflection, no preferred direction of re-emission exists, thus only the normal force exists. The pressure due to diffuse reflection for a flat plate wing is given by^{15,16}

$$P_r = \frac{\sqrt{\pi}}{2} C (M_r^{\text{trans}} | M_r^{\text{refl}}) \quad (23)$$

where the pressure due to diffuse reflection is dependent on which side of the wing is in the shadow, as defined by the "I" (OR) symbol, and

$$C = \sqrt{2 R T_r} = \frac{1}{B} \quad (24)$$

$$M_r^{\text{trans}} = \rho_a \int_{-\infty}^{\infty} \int_{-\infty}^{\infty} \int_0^{\infty} (C_r \cdot \hat{n}) f(C_r - v_{w/O} + \omega \times r) dC_r \quad (25a)$$

$$M_r^{\text{refl}} = -\rho_a \int_{-\infty}^{\infty} \int_{-\infty}^{\infty} \int_0^{\infty} (C_r \cdot \hat{n}) f(C_r - v_{w/O} + \omega \times r) dC_r \quad (25b)$$

For this problem it is assumed $T_i = T_r = T$, the free stream temperature, and the plate encounters steady state reflection.

To determine the total moment about the tether-TS/WS connection for one wing, we use the relationship

$$M = \int_s r \times (P_i + P_r) dS \quad (26)$$

and then integrate eqn (26) for each wing, linearizing, and summing the results for all four wings, we obtain the total aerodynamic moments due to the wings (M_w).

Objective Function Development and Constraint Identification

The differential equations used to derive the equations of motion of the TS/WS is given by setting the left hand side of eqn. (7) equal to $M_g + M_{dp} + M_w$. Examination of the differential equations first shows that the gravity gradient effects about the roll and pitch axis are 2 orders of magnitude larger than the effects from the horizontal wings, hence the horizontal wings can be removed from the model. Also in the differential equations there is a coupling of the Euler angles (Ψ, γ, ϕ) with the velocity of the atmosphere which in turn is a function of angular position of the TS/WS in the orbit. In order to derive an analytic solution to the differential equation, we considered the case when $i=0^\circ$. In order to test the optimal solution, the behavior of the TS/WS when $i=29^\circ$ was examined to confirm the system remains oriented within the required tolerances and is stable.

Further examination of the differential equations shows that the aerodynamic damping terms are very small and hence negligible in effect. Thus, the aerodynamic damping terms can be removed from the analysis. Note, by doing this, the TS/WS has no means to dampen its motion. In order to provide energy dissipation in the model, we included in the design an arbitrary damping term, ζ , which can physically be modeled through the use of one or more nutation dampers (nutation dampers typically consist of a mass-spring system in a fluid-filled tube). Though the damping term is defined by the characteristics of the nutation damper, since the damper was not included in the physical model, for the purposes of this paper it was treated as an arbitrary value. Note, for all $\zeta > 0$ the peak overshoot about each axis is always less than the undamped maximum amplitude. Thus we can simplify the problem by optimizing based on the undamped system; later, damping was applied to the optimal solution to examine its effects.

Collecting terms and dividing by $1/2 \rho_a S_w v_o^2 d_{OB}$ and then multiplying by the inverse of the inertia dyadic, the equations of motion are given by

$$I \begin{Bmatrix} \ddot{\Psi} \\ \ddot{\phi} \\ \ddot{\gamma} \end{Bmatrix} + \begin{Bmatrix} 0 & -\Gamma_x & 0 \\ \Gamma_y & 0 & 0 \\ 0 & 0 & 0 \end{Bmatrix} \begin{Bmatrix} \dot{\Psi} \\ \dot{\phi} \\ \dot{\gamma} \end{Bmatrix} + \begin{Bmatrix} \omega_\Psi^2 & 0 & 0 \\ 0 & \omega_\phi^2 & 0 \\ 0 & 0 & \omega_\gamma^2 \end{Bmatrix} \begin{Bmatrix} \Psi \\ \phi \\ \gamma \end{Bmatrix} = \begin{Bmatrix} -\kappa \text{sign}(\psi) \\ 0 \\ 0 \end{Bmatrix} \quad (27)$$

where

$$\Gamma_\phi = \left(1 + \frac{I_{yy}^O}{I_{xx}^O} - \frac{I_{zz}^O}{I_{xx}^O} \right) \theta \quad (28)$$

$$\Gamma_\psi = \left(1 + \frac{I_{xx}^0}{I_{yy}^0} - \frac{I_{zz}^0}{I_{yy}^0} \right) \theta \quad (29)$$

$$\omega_\psi^2 = \frac{1}{\mu_{xx}^0 d_{OB}^2} \left[\frac{R}{B\sqrt{\pi}} (2 + \pi) - C_{d_p} \frac{S_p}{S_w} \frac{d_{AO}}{d_{OB}} R^2 \theta \right] (\theta - \Omega) + \left(\frac{I_{zz}^0}{I_{xx}^0} - \frac{I_{yy}^0}{I_{xx}^0} \right) 2\theta^2 \quad (30)$$

$$\omega_\phi^2 = \frac{1}{\mu_{yy}^0} \left[\left(\mu_{xx}^0 - \mu_{xx}^0 \right) \left(2\theta^2 + 3 \frac{\mu}{R^3} \right) + \frac{m R d_{OC}}{2 \rho_a S_w d_{OB}^3} \left(\frac{\mu}{R^3} - \theta^2 \right) \right] \quad (31)$$

$$\omega_\gamma^2 = \frac{1}{\mu_{zz}^0} \left[\left(\mu_{yy}^0 - \mu_{xx}^0 \right) \left(2\theta^2 + 3 \frac{\mu}{R^3} \right) + \frac{m R d_{OC}}{2 \rho_a S_w d_{OB}^3} \left(\frac{\mu}{R^3} - \theta^2 \right) + \frac{1}{d_{OB}^2} \left[\frac{2R}{B\sqrt{\pi}} - C_{d_p} \frac{S_p}{S_w} \frac{\theta}{d_{OB}} \left(d_{AO}^2 + 2d_{AO} r_p + d_{AO} (r_p^2 + R^2) \right) \right] \right] (\theta - \Omega) \quad (32)$$

$$\mu^0 = \frac{I^0}{\frac{1}{2} \rho_a S_w d_{OB}^3} \quad (33)$$

$$\kappa = \frac{\rho S_w d_{OB}}{B^2 I_{xx}^0} \quad (34)$$

Note, from eqn (14), $d\theta/dt \neq \mu/R^3$.

Since the system being optimized is not damped and the amplitude of motion is constant, we need only to optimize on the modal, or natural, frequencies of the TS/WS. However, because $\omega_\psi^2 \ll \omega_\phi^2, \omega_\gamma^2$, the natural frequency about the yaw axis is effected most by the variation of ω_ψ^2 . Furthermore, investigation of the stiffness terms shows that variation of the design parameters primarily influences the yawing stiffness term. Since motion about the yaw axis is impacted by the inclination of the orbit (i.e. effects due the the relative velocity of the atmosphere, or crosswind, due to Earth's rotation) eqn (30) was selected as the objective function to minimize. (Note, alternatively one could have considered taking the sum of the squares of the modal frequencies as the objective function to minimize).

The necessary and sufficient conditions for optimization are that the system is stable and the TS/WS point in the direction of the velocity vector to within a tolerance of 2° . To satisfy the latter condition, one can determine a range of initial conditions through simple numerical means such that the required tolerances are met. In considering the former condition, if we assume homogeneous solutions to eqn (26) of the form

$$x = A C e^{\lambda t} \quad (35)$$

and substitute back into eqn (26), we obtain

$$\left(\mathbf{1} \lambda^2 + \begin{bmatrix} 0 & -\Gamma_\psi & 0 \\ \Gamma_\psi & 0 & 0 \\ 0 & 0 & 0 \end{bmatrix} \lambda + \begin{bmatrix} \omega_\psi^2 & 0 & 0 \\ 0 & \omega_\phi^2 & 0 \\ 0 & 0 & \omega_\gamma^2 \end{bmatrix} \right) \mathbf{A} = 0 \quad (36)$$

from which the characteristic equation for the system can be obtained (and a solution to eqn (35) can be determined). For the system to be stable, we require the eigenvalues λ^2 are negative and real and distinct.²² From eqn (36) we find the necessary and sufficient conditions for stability are

$$\left. \begin{aligned} \lambda_{1,2,3,4}^2 &= \left\{ -\Gamma_\psi \Gamma_\psi - \omega_\psi^2 - \omega_\phi^2 \pm \left(\Gamma_\psi \Gamma_\psi + \omega_\psi^2 - 2\omega_\psi \omega_\phi + \omega_\psi^2 \right)^{1/2} * \right. \\ &\quad \left. \left(\Gamma_\psi \Gamma_\psi + \omega_\psi^2 + 2\omega_\psi \omega_\phi + \omega_\psi^2 \right)^{1/2} \right\} / 2 < 0 \\ \lambda_{5,6}^2 &= -\omega_\gamma^2 < 0 \\ \lambda_{1,2}^2 &= \lambda_{3,4}^2 = \lambda_{5,6}^2 \end{aligned} \right\} \quad (37)$$

and $\lambda_{i,i+1}^2 \in \mathfrak{R}$, where $i=1,3,5$.

In reference 4 the design variables to be optimized were the boom length, the wing inclination and the wing area. It was found that the optimal values were for a maximum wing area and boom length and a wing inclination of 0° . In this model we will retain the wing area and boom length (d_{OB}) as design variables, and will fix the boom length at its maximum allowable length and maintain the wing inclination at 0° . A list of the design variables to be optimized is given in table 1. These design variables are used to minimize the objective function.

The constraints are:

- g1: $\lambda_{1,2}^2 < 0$
- g2: $\lambda_{3,4}^2 < 0$
- g3: $\lambda_{5,6}^2 < 0$
- g4: $\text{rank}(\mathbf{U}) = 6$
- g5: $d_s > 1/2$
- g6: $d_s > 0.9$
- g7: $d_s \leq 1.85 \text{ Cos} [\text{Sin}^{-1} (1/3.7)]$
- g8: $l \geq 0.32$

Table 1 Design Variables used for Optimization

d_b	l
r_b	d_k
ρ	m_k
d_s	

g9:	$l \leq 2.236$
g10:	$d_{AO} > 0.1 d_b + r_p$
g11:	$m \leq 610$
g12:	$m > 500$
g13:	$d_k < 2$
g14:	$d_k > 0$
g15:	$r_b > 0$
g16:	$r_b \leq 0.03$

The constraints g1 - g3 require the necessary and sufficient conditions for stability be met. g4 requires the TS/WS be controllable about all three body axes. Constraints g5 - g9 specify the space available to the boom-wing structure in the shuttle cargo bay. The constraint g10 insures there is no contact between the tether and the spherical probe of the tethered satellite. Constraints g11 and g12 are mass constraints. g13 specifies the maximum length of the "keel" structure; g14 indicates the keel structure must exist to have roll control. Lastly, g15 and g16 are geometric constraints related to the radius of the boom structure.

A parametric study shows that g3 is never violated for all feasible values of the variables listed in table 1. Since g14 must never be violated, the rank of the controllability matrix will always satisfy g4. Hence g3 and g4 can be removed from the computation. In general, it would be prudent to test any "optimal" design to be sure that the removed constraints are satisfied.

IV. Model Solution

Table 2 lists the parameters used in determining the optimal configuration for the TS/WS. Using the parameters listed $v_o = 7,359$ m/s.

Table 2 System Parameters used in Optimization

Parameter	Value
C_{Dp} (ref. 6)	2.1
r_p	0.8 m
r_s	0.025 m
r_k	0.025 m
l	0.01 l
h_o (ref. 6)	230×10^3 m
$h_{ts/ws}$	142×10^3 m
i	0°
α	6378.14×10^3 m
Ω	$7.250 \times 10^{-5} \text{ s}^{-1}$
μ	$3.986 \times 10^{14} \text{ m}^3 \text{ s}^{-2}$
ρ_a (ref. 23)	$3.358 \times 10^{-9} \text{ kg m}^{-3}$
T (ref. 23)	575.7° k

The optimal configuration was found using the computer application *Optimum*.²⁰ *Optimum* is a FORTRAN program which incorporates the general conjugate gradient and golden section acceptable point search algorithm in finding the optimal solution for a given objective function and set of constraints. In order to code the objective function and the constraints, an analytic model of the TS/WS as discussed in section III was developed using *Mathematica*.¹⁹ Once developed, FORTRAN code was then generated through use of the command FortranForm, and then then resulting code was "pasted" into the program *Optimum*. Using the modified code, a numerical optimal solution was found for ω_{nv}^2 , which satisfies the necessary and sufficient conditions for stability. Those results are presented in table 3. Note that ζ was arbitrarily set to 0.1. Figure 5 shows a detailed conceptual model of the optimal design.

Table 3 Optimal TS/WS Configuration

Variable	Result
d_b	6 m
r_b	0.03 m
l	1.9 m
d_k	1.5 m
m_k	15 kg
d_s	1.59 m
ζ	0.1
ρ (titanium)	4377 kg/m^3

Table 4 Range of Allowable Initial Conditions

$$|\psi(0), \gamma(0)| < 1.5^\circ$$

$$|\phi(0)| < 5^\circ$$

$$|(d\phi/dt)_0, (d\gamma/dt)_0, (d\psi/dt)_0| < 0.001175 \text{ rads/secs}$$

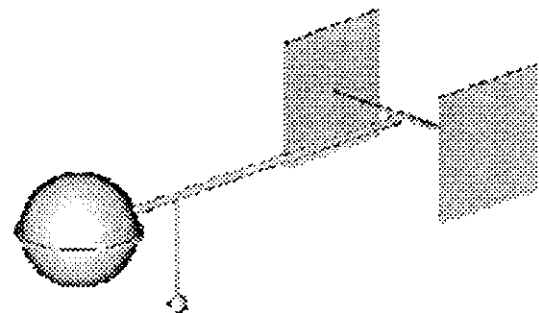


Fig. 5 Detailed conceptual model of the optimal configuration of the TS/WS.

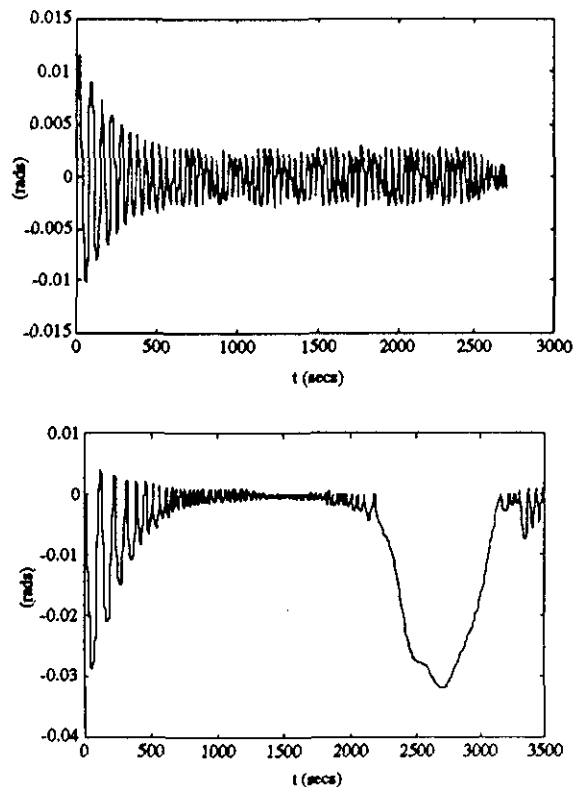


Fig. 6 Motion of the TS/WS about the yaw (x) axis for $i=0^\circ$ (upper plot) and $i=29^\circ$ (lower plot).

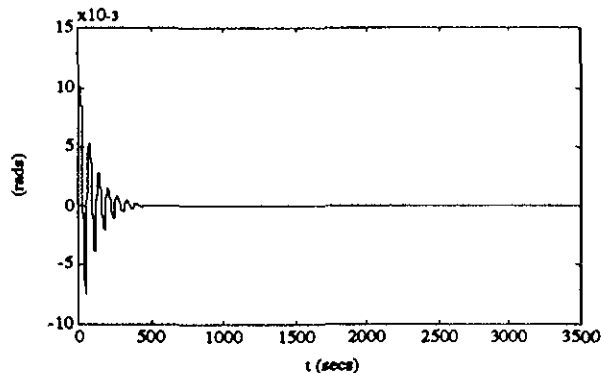


Fig. 7 Motion of the TS/WS about the pitch (z) axis for $i=29^\circ$ (note — the crosswind has a negligible effect on the pitching motion).

For comparison, the objective function was also examined graphically by varying the design parameters using *Mathematica*. The graphical results do correlate with the results obtained in *Optimum*. Through graphical analysis, using the application *Matlab*, the range of allowable initial conditions were also determined such that the TS/WS is oriented towards the velocity vector within the given tolerances. These results are presented in table 4.

As indicated earlier, we also wanted to study the effects of orbital inclination on the TS/WS. Figures 6 and 7 show the

effects of orbital inclination on yaw, roll and pitch respectively. In all plots $\theta(0) = \psi(0) = \phi(0) = \chi(0) = (d\theta/dt)_0 = (d\psi/dt)_0 = 0$, $(d\psi/dt)_0 = 0.001175$ rads/sec, $i=0,29^\circ$. Note the effects of the crosswind on the yaw motion — the cross wind acts as a varying forcing function about the yaw axis for inclined orbits and the peak displacement will always occur at the equator.

V. Future Work

In the future several additional tasks will be addressed. The primary task will be to develop an aerodynamic model of the TS/WS in the transition flight regime (Knudsen numbers between 1 - 10) and to develop models of the TS/WS flight characteristics. Though little detail is still known about the Thermosphere, Bird has developed a technique known as the *Direct Simulation Monte Carlo Method* (DSMC) for accurately modeling on a computer gas flows over surfaces.⁹ The software will be used to determine the lift, drag and moment coefficients, aerodynamic heating, and flow characteristics of the TS/WS. The target goal of this task will be to develop a mathematical model defining the behavior of the TS/WS which can be integrated into the dynamic model.

Since we will be considering transitional effects, one can anticipate that the spherical probe will effect the atmospheric flow at the wings. To account for this effect we will reintroduce the wing inclination as a design parameter.

We would also like to consider other configurations of the TS/WS, including modeling the system with the tether connected to the sphere and removing the keel structure. Once completed a comparison study will be conducted between the various configurations in the transition and free molecular flow flight regime. With all these modifications it is anticipated the set of constraints will need modification, plus a variety of new constraints and design variables will be added as required. It is hoped at the completion of the analytic modeling and analysis we can test the results by experimentation via ground based labs.

VI. Conclusion

These results indicate that an appropriately configured passive wing system could provide stable flight for a TS/WS in free molecular flow subject to a variety of initial conditions. As a result, sensing probes on the satellite could accurately measure and study the Earth's upper atmosphere. In showing the feasibility of a passive wing system, an inexpensive alternative for TSS control can be considered versus the expense and complexity of an active control system. As indicated, the next step will be to investigate the behavior of the system in transitional flow and alternative configurations.

References

- 1 Anderson, J. L., "Outer Atmospheric Research Using Tethered Systems", *Journal of Spacecraft and Rockets*, Vol. 26, March-April 1989, pp. 66-71.

- 2 NASA, "Tethered Satellite System 2", May 1989, NASA OAST, Washington D.C.
- 3 NASA Technical Memorandum, "Shuttle/Tethered Satellite System Conceptual Design Study", NASA TM X-73365, December 1976.
- 4 Facility Requirements Definition Team Report, "Tethered Satellite System Facility Requirements", April 1980
- 5 Santangelo, A.D. and Johnson, G. E., "Optimal Wing Configuration of a Tethered Satellite in Free Molecular Flow", 30th AIAA Aerospace Sciences Meeting, AIAA 92-0218, Washington D.C., January 1992.
- 6 Johnson, J. D., private communication, "Drag on the Proposed Tethered Satellites", 1979, Marshall Space Flight Center, Huntsville, Alabama
- 7 Johnston, K.D., "Aerodynamics", *Tethered Subsatellite Study*, NASA TM X-73314, March 1976
- 8 Dogra, V.K. and Wilmoth, R.G. and Moss, J.N., "Aerothermodynamics of a 1.6 m Diameter Sphere in Hypersonic Rarefied Flow", 29th Aerospace Sciences Meeting and Conference, AIAA 91-0773, Washington D.C., January, 1991
- 9 Dogra, V.K. and Moss, J.N. and Wilmoth, R.G. and Price, J.M., "Hypersonic Rarefied Flow Past Spheres Including Wake Structure", 30th Aerospace Sciences Meeting and Conference, AIAA 92-0495, Washington D.C., January, 1992
- 10 Dogra, V.K. and Moss, J.N., "Hypersonic Rarefied Flow About Plates at Incidence", *AIAA Journal*, Vol.29, No. 8, August 1991, pp. 1250 - 1258.
- 11 Longuski, J.M. and Puig-Suari, J., "Modeling and Analysis of Orbiting Tethers in an Atmosphere", AIAA/AAS Astrodynamics Conference, AIAA-90-2897, Washington, D.C., August, 1990.
- 12 Longuski, J.M. and Puig-Suari, J., "Hyperbolic Aerocapture and Elliptical Orbit Transfer Tethers", 42nd Congress of the International Astronautical Federation, IAF-91-339, Montreal, Canada, October, 1991.
- 13 Fujii, H. and Kokubun, K. and Uchiyama, K. and Saganuma, T., "Deployment/Retrieval Control of a Tethered Subsatellite under Aerodynamic Effect of Atmosphere", *The Journal of the Astronautical Sciences*, Vol.40, No. 2, April-June 1992, pp. 171 - 188.
- 14 Shakhov, E.M., "Oscillations of a Tethered Satellite", *Rarefied Gas Dynamics*, Vol. 117, AIAA, Washington, D.C., 1989, pp. 42-52.
- 15 Blick, E.F., "Forces on Bodies of Revolution in free molecular flow by the newtonian-diffuse method", 1959, St. Louis, Mo, 6670, McDonnell Aircraft Corporation.
- 16 Bird, G.A., *Molecular Gas Dynamics*, Clarendon Press, Oxford, 1976.
- 17 Shidlovskiy, V.P., *Introduction to Dynamics of Rarefied Gases*, American Elsevier Publishing Company, New York, 1967.
- 18 Kennedy, G. P. & Joels, K. M., *The Space Shuttle Operator's Manual*, Ballantine Books, New York, 1982.
- 19 Wolfram, S., *Mathematica*, Addison-Wesley Publishing Company, Redwood City, CA, 1988.
- 20 Johnson, G.E. and Townsend, M.A., "An Acceptable-Point Algorithm for Design Optimization", *Optimal Design of Mechanical Elements*, Wiley Interscience, New York, 1980, pp.488-507.
- 21 Beletskii, V., "Motion of an Artificial Satellite About its Center of Mass", ---**
- 22 Greenwood, D.T., *Classical Dynamics*, Prentice-Hall, Inc. Englewood Cliffs, N.J., 1977.
- 23 NASA, NOAA and USAF, *U.S. Standard Atmosphere, 1976*, Washington D.C.